IDSA
Infectious Diseases Society of America

hivma
hiv medicine association

OXFORD

C1q Confers Protection Against Cryptococcal Lung Infection by Alleviating Inflammation and Reducing Cryptococcal Virulence

Xu Zhao,[1,*] Lei Shen,[2,*] Jianming Zheng,[2,*] Haiyan Zhu,[3] Li Li,[4] Hong Shi,[5] Zhongqing Chen,[6] and Qian Li[2,]

[1]Institute of Antibiotics, Huashan Hospital, Fudan University, Shanghai, China, [2]Department of Infectious Diseases, Shanghai Key Laboratory of Infectious Diseases and Biosafety Emergency Response, National Medical Center for Infectious Diseases, Huashan Hospital, Fudan University, Shanghai, China, [3]Department of Biological Medicines & Shanghai Engineering Research Center of ImmunoTherapeutics, School of Pharmacy, Fudan University, Shanghai, China, [4]Laboratory of Mycology, Department of Dermatology, Huashan Hospital, Fudan University, Shanghai, China, [5]Department of Anesthesiology, Shanghai Pulmonary Hospital, School of Medicine, Tongji University, Shanghai, China, and [6]Department of Pathology, Huashan Hospital, Fudan University, Shanghai, China

Background. To define the role of C1qa in host defense against *Cryptococcus neoformans* lung infection, we investigated its susceptibility to cryptococcal lung infection in mice deficient in complement factor C1qa ($C1qa^{-/-}$).

Methods. We established a wild-type (WT) and C1qa-deficient murine inhalation model with *C. neoformans*. We compared the host survival rate, inflammatory responses, and pathogenicity of *C. neoformans* during the infection course between WT and $C1qa^{-/-}$ mice.

Results. The mortality rate of C1qa-deficient mice was significantly higher than that of wild-type mice. The increased formation of Titan cells in the lungs was associated with augmented inflammation in C1qa-deficient mice. The capacity of lung homogenate supernatant from C1qa-deficient mice to induce Titan formation in vitro was greater compared with that of wild-type mice. The *C. neoformans* isolated from the lungs of infected C1qa-deficient mice was more resistant to macrophage killing in vitro and caused significantly higher mortality after administration to mice compared with that isolated from WT mice.

Conclusions. These findings reveal a novel role of C1qa in host defense against *C. neoformans* infection by regulating host inflammation and pathogen virulence and provide new insight into the C1q-mediated lung environment underlying the transition from yeast to Titan cell.

Keywords. C1q; *Cryptococcus neoformans*; inflammatory response; Titan cells.

Cryptococcus neoformans mostly occurs in immunocompromised individuals, and infection often leads to pulmonary cryptococcosis and cryptococcal meningitis or meningoencephalitis, which cause high rates of mortality [1]. Alteration of morphology is a common feature of *C. neoformans* that favors its survival and persistence in the host during infection [2, 3]. Specifically, in response to the host environment, *C. neoformans* changes its morphology and generates enlarged cells referred to as giant or "Titan" cells, which have been observed

in different *Cryptococcus* infection models and human clinical samples [4, 5]. By altering the morphology from the typical 5–7-μm size of cells to Titan cells ranging from 10 μm up to 100 μm, *C. neoformans* enhances its virulence and increases its ability to disseminate and survive [6]. To date, many host-related factors, including nutrient deprivation, pH, and hypoxia, have been identified to influence the alteration of *C. neoformans* morphology during infection [7]. However, fewer immune defense factors that contribute to the alteration of *C. neoformans* morphology have been identified [8].

The complement system, a vital component of the innate immune system, plays an important role in protecting the host against infections. There are 3 pathways, including the classical, alternative, and lectin pathways, that can individually activate the complement system [9]. C1q, in addition to being the recognition molecule of the classical pathway, is able to directly identify a series of self or nonself ligands through its head domain (gc1q) or through immunoglobulin (Ig)G and C-reactive protein (CRP) [10]. This links innate immunity with adaptive immunity. In recent years, new research findings have shown that C1q performs a diverse range of noncomplement functions. It can mediate a variety of immune regulatory functions, including modulating the functions of immune

and nonimmune cells [11], regulating the production and secretion of cytokines, and preventing the enhancement of autoimmune phagocytosis [12, 13]. However, little information exists concerning the role of C1q in mediating inflammatory response during *C. neoformans* infection in vivo.

In this study, we used a mouse model of lung infection to investigate the impact of C1qa deficiency on host disease outcome, inflammatory response, and cryptococcal virulence during the disease course. Our results show that deficiency in C1q did not influence the growth/translocation of the cryptococci in the host, but it enhanced inflammatory response as well as lung damage, which was associated with increased virulence of the cryptococci in mice.

METHODS

Ethics Statement

All animals used in this study were treated according to the standards set out in the Ethical Principles Guide for the Care and Use of Laboratory Animals, which was adopted by the Fudan University Animal Care and Use Committee guidelines. The Committee of Ethics in Animal Research of Fudan University approved the protocols (Protocol 2021JS Huashan-070).

Mice and *C. neoformans*

C57BL/6 wild-type (WT) mice were obtained from Shanghai Model Organisms Center, Inc. $C1qa^{-/-}$ mice were originally developed by Marina Botto and subsequently back-crossed on a C57BL/6 background [14, 15]. We obtained a breeding pair of $C1qa^{-/-}$ mice from Laura E. Nagy at the Department of Pathobiology, Lerner Research Institute, Cleveland, Ohio, and utilized them to establish a breeding colony at the Shanghai Model Organisms Center.

The *C. neoformans* H99 strain was generously provided by our colleague, Dr. Liping Zhu, and cultured on yeast extract-peptone-dextrose (YPD) agarose plates for 48 hours at 30°C. The yeast cells were then resuspended in sterile PBS at a concentration of 2×10^6 yeast cells/mL before use. We used 20 µL of the cell suspension containing 4×10^4 yeast cells for intranasal inoculation per mouse (4×10^4 yeast cells per mouse).

Intranasal Infection With *C. neoformans*

Male WT and $C1qa^{-/-}$ mice aged 8–10 weeks were anesthetized with xylazine (125 mg/kg) and ketamine (10 mg/kg) before intranasal inoculation with 4×10^4 yeast cells per mouse [16]. On days 1, 7, and 14 post–*Cryptococcus* infection, mice in each group were killed. We fixed half of the left lung lobes of the mice in 4% formalin for pathological examination. The other half of the left lung was used for flow cytometry to detect inflammatory cells. The lung tissues were cut into 2×4-mm pieces and ground. The cell suspensions were then passed through a 70-µm filter. We aseptically removed the right lung lobes, liver, brain, and spleen and homogenized them in sterile normal saline. The tissue homogenates were serially diluted and plated for counting. The *C. neoformans* burden in each organ was expressed as CFU/mg. We centrifuged the lung homogenates at 300×*g* for 5 minutes to obtain the supernatant. For survival studies, we intranasally instilled WT (n = 12) and $C1qa^{-/-}$ (n = 18) mice with 4×10^4 yeast cells or sterile PBS. We monitored the mice every day for 42 days postinfection, at which time all of the $C1qa^{-/-}$ mice had died.

Cytokine Measurements in Tissues

The cytokines in the lung homogenate supernatant of mice were measured using enzyme-linked immunosorbent assay kits, including TNF-α (CSB-E04741m), IL-10 (CSB-E04594m), IFN-γ (CSB-E04578m), IL-12/p70 (CSB-E04600m), IL-6 (CSB-E04639m), IL-17A (CSB-E04602m), IL-1β (CSB-E08054m), CXCL1 (JL20150), IL-13 (JL20247), MCP-1 (JL20304), and IL-1α (JL13044), according to the manufacturer's protocol. The cytokine concentrations were determined using a standard curve and expressed as pg/mL.

Histology

The formalin-fixed lung tissues from WT and $C1qa^{-/-}$ mice infected with *C. neoformans* were dehydrated, paraffin-embedded, sectioned at a thickness of 4 µm, and stained with hematoxylin and eosin, as previously described [17]. The lung histopathological score, including infiltrating inflammation cells, was determined as previously described (Supplementary Table 1 and Figure 1) [18, 19]. *Cryptococcus* burden and morphology in the lung were observed under a microscope.

Characterization of Yeast Cell Morphology and Determination of the Virulence of *Cryptococcus* Isolated From $C1qa^{-/-}$ and WT Mice

To visualize the cryptococcal capsule and size, prototype yeast cells H99 were incubated with lung homogenate supernatant from infected WT and $C1qa^{-/-}$ mice for 72 hours. In addition, we used 10% fetal calf serum (FCS) to induce Titan cells [20] with or without human C1q protein (Quidel, A400) at a final concentration of 100 µg/mL to observe the direct effect of C1q protein on cryptococcal titanization. Live cells were counterstained using India Ink, and their diameter was measured using NIS-Elements D Imaging Software (Nikon, Japan). Eight images per sample were randomly selected, and 100 cells in these selected images were used to quantify yeast cell capsule and size.

The lung homogenates from $C1qa^{-/-}$ and WT mice, 14 days after cryptococcal infection, were cultured at 30°C for 48 hours. Yeast strains, isolated from WT and $C1qa^{-/-}$ mice, were referred to as the WT isolate and knockout (KO) isolate, respectively. Their size was examined as described above. To

assess whether the morphology alteration was associated with its virulence, WT mice (n = 7) were intranasally infected with the WT isolate or KO isolate of *Cryptococcus* with 2×10^4 yeast cells per mouse and monitored for survival for 42 days postinfection.

Macrophage Killing Assays

THP-1 cells were treated with phorbol 12-myristate 13-acetate (PMA) at a concentration of 100 ng/mL for 2 hours to generate a macrophage-like phenotype. These PMA-induced THP-1 macrophages were seeded into a 48-well plate at a density of 2×10^5 cells per well and cultured for 24 hours at 37°C before adding LPS (200 ng/mL). After 18 hours of LPS stimulation, the activated macrophages were incubated with yeast cells, including the prototype H99, KO, or WT isolate at a concentration of 2×10^6 yeast cells/mL. For the macrophage killing assay, 10 μL of yeast cells (2×10^4 yeast cells) were inoculated into wells containing activated macrophages. After incubation for 18 hours at 37°C, the culture supernatant was removed, and 200 μL of ddH$_2$O was added to each well to lyse the macrophages. The supernatant and lysate were then plated on YPD agarose plates; *C. neoformans* cells were grown for 48 hours at 30°C and counted.

Immunofluorescence Staining

The lung sections described above were deparaffinized using the standard protocol. After antigen retrieval, the slides were stained with primary antibodies including CD4 antibody (SB 50134 -R766, 1:50), CD8 antibody (CST 98941 seconds, 1:20), and F4/80 antibody (CST 7076 seconds, 1:500) for 1 hour at room temperature. Then, the slides were incubated with fluorescent-labeled secondary antibodies (1:500) for 1 hour at room temperature. Lastly, the slides were stained with DAPI and mounted before being visualized and photographed. One hundred cells in each sample were randomly selected to calculate the proportion of CD4-, CD8-, and F4/80-positive cells.

Detection of Inflammatory Cells in the Lungs by Flow Cytometry

The lung cell suspensions were centrifuged at 300×*g* for 5 minutes to obtain the cell pellet. Approximately 1×10^6 cells per sample were stained with Fixable Near-IR Live/Dead (Invitrogen, L34975) and monoclonal antibodies (CD45-BV510 [BD, 2154345], CD4-PE-CY7 [BD, 552775], CD8a-PerCP-Cy5.5 [BD, 551162], F4/80-PE [BD, 2165051]) for 30 minutes at 4°C. The stained cells were fixed in 1.5% paraformaldehyde for 5 minutes and analyzed using a Cytoflex S flow cytometer (Beckman). The data were analyzed with FlowJo software.

Statistical Analysis

The unpaired samples' *t* test (2-tailed) or 1-way analysis of variance using GraphPad Prism, version 9.0, for Windows (GraphPad Software, San Diego, CA, USA) was used to detect statistically significant differences, defined as $P < .05$. The log-rank test was used for survival analysis.

RESULTS

C1qa-deficient mice were more susceptible to *C. neoformans* infection despite having a similar pathogen load compared with wild-type mice.

In our previous studies, we showed that complement components, including C1q, were significantly increased in the CSF of cryptococcal meningitis patients [21]. To investigate the role of C1q during *C. neoformans* infection, we used a murine inhalation model of cryptococcal infection. We intranasally instilled 4×10^4 *C. neoformans* CFUs in WT and *C1qa*$^{-/-}$ mice and determined their survival rate. We found that *C1qa*$^{-/-}$ mice displayed significantly higher mortality compared with WT mice. Both WT and *C1qa*$^{-/-}$ mouse deaths began at 16 days, and all *C1qa*$^{-/-}$ mice succumbed to death at 23 days postinfection, whereas only 50% of WT mice died. Thus, C1qa-mediated effects contributed to mouse survival during *C. neoformans* infection (Figure 1A).

One possible reason for this observation is that C1qa-mediated effects create adverse conditions for the growth and/or translocation of *C. neoformans* during infection. To explore these possibilities, we infected WT and *C1qa*$^{-/-}$ mice with 4×10^4 *C. neoformans* and killed them at days 1, 7, and 14 postinfection. We determined fungal loads in the lungs from their homogenates by plate counting. Our data showed that *C. neoformans* growth in lungs was similar in both groups of mice within 2 weeks of infection (Figure 1B).

Next, we sought to determine whether *C1qa* deficiency influenced *C. neoformans* translocation to other organs. While *C. neoformans* was detected in the brain, spleen, and liver of both groups of mice, there were smaller numbers of *C. neoformans* in these organs than in the lungs of both WT and *C1qa*$^{-/-}$ mice. Compared with WT mice, *C1qa*$^{-/-}$ mice had a slightly increased number of *C. neoformans* in the brain, spleen, and liver, but this difference did not reach statistical significance (Figure 1C). Our data demonstrated that, despite a similar pathogen load in the lungs, C1qa deficiency resulted in increased susceptibility to *C. neoformans* infection, indicating a critical role of C1qa in the host defense against this pathogen.

C. neoformans Infection Causes More Severe Inflammatory Pathology in *C1qa*$^{-/-}$ Mice Than in WT Mice

Despite having similar *C. neoformans* loads in the lung, the analysis of lung pathology by HE staining showed that the inflammatory pathological changes characterized by peribronchiolar/bronchial infiltrates and destructed lung tissue were more severe in *C1qa*$^{-/-}$ mice than in WT mice (Figure 2). Specifically, *C1qa*$^{-/-}$ mice exhibited a more extensive bronchiolar/bronchial luminal exudate and nearly confluent
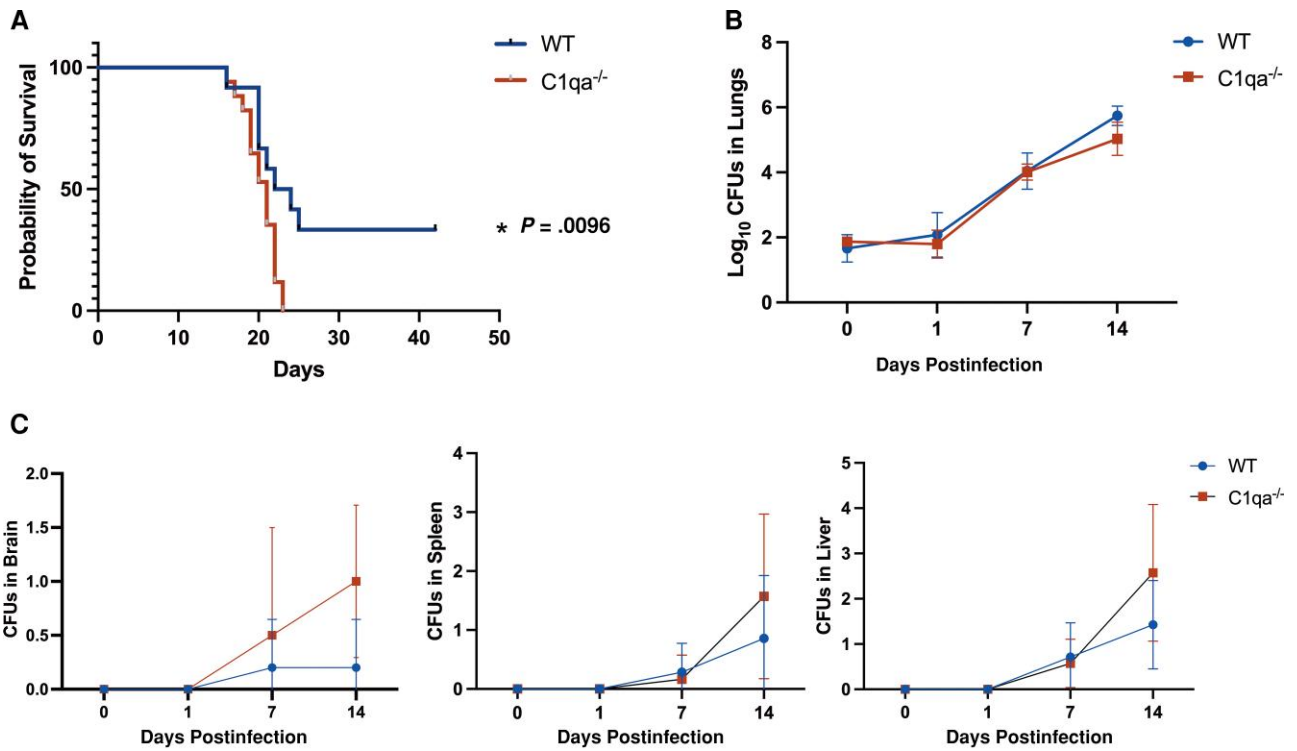
Figure 1. C1qa-mediated effects contributed to mouse survival but not fungal burden or distribution during infection. *A*, *C1qa*$^{-/-}$ and WT mice were intranasally instilled with 4×10^4 *C. neoformans* CFUs and monitored for survival until 23 days postinfection. *B* and *C*, Homogenized organs ([*B*] lungs; [*C*] brain, spleen, and liver) on days 1, 7, and 14 postinfection were serially diluted and plated on YPD agarose plates. Colonies were counted as CFU/mg. Abbreviations: CFUs, colony-forming units; WT, wild-type; YPD, yeast extract-peptone-dextrose.

peribronchiolar/bronchial infiltrate compared with WT mice, which only showed moderate peribronchial cuffing (Figure 2A–D). Multiple well-demarcated nodular lesions were present in WT mice, which were more severe in *C1qa*$^{-/-}$ mice (Figure 2A). *C1qa*$^{-/-}$ mice also showed a modest, nonsignificant increase in perivascular infiltrate compared with WT mice (Figure 2E, F). The overall histopathological scores, based on the criteria in Supplementary Table 1 and Figure 1, further confirmed that there was more severe inflammatory lung pathology in *C1qa*$^{-/-}$ mice during *C. neoformans* infection (Figure 2G).

C. neoformans Infection Causes Enhanced Inflammatory Immune Response in *C1qa*$^{-/-}$ Mice

To characterize the pro-inflammatory cytokines, lymphocyte, and macrophage infiltrate that may be associated with pathological changes following *C. neoformans* infection, we analyzed the inflammatory cytokines, including IL-6, IL-12, INF-γ, IL-17A, IL-1β, IL-1α, IL-13, CXCL1, MCP-1, CD4/CD8 T cells, and macrophages in the lungs of WT and *C1qa*$^{-/-}$ mice during *C. neoformans* infection. IL-6 is a proinflammatory cytokine induced at the early stage of infection, while IL-12 often has a significant impact on the late stage of inflammation and is closely related to lymphocyte immune response and crucial for

phagocyte activation. Measurement of the expression of IL-6 and IL-12 in the lung supernatant showed that compared with WT mice, *C1qa*$^{-/-}$ mice presented significantly higher levels of IL-6 on days 1 and 7 postinfection (Figure 3A) and displayed enhanced IL-12 expression on days 1 and day 14 postinfection (Figure 3B). The measurement of Il-17A in the lung supernatant showed that it was slightly higher in WT mice compared with *C1qa*$^{-/-}$ mice on day 1 postinfection (Figure 3C). In an analysis of CD4, CD8 T cells, and macrophages by immunofluorescence staining and flow cytometry, both methods showed that the number of CD4 T cells in the lungs of *C1qa*$^{-/-}$ mice was significantly higher than that in WT mice, while the level of CD8 T cells and macrophages were comparable between these 2 groups (Figure 4). In summary, compared with WT mice, *C1qa*$^{-/-}$ mice displayed a modest increase of some inflammatory cytokines and immune cells in the lung following *C. neoformans* infection.

Microenvironment in the Lungs of *C1qa*$^{-/-}$ Mice Favors the Generation of Titan Cells During *C. neoformans* Infection

It has been reported that *C. neoformans* changes its morphology from haploid to highly polyploid cells termed Titan cells in the host lung, and these morphogenic transitions often lead to increased virulence in *C. neoformans*, consequently enhancing
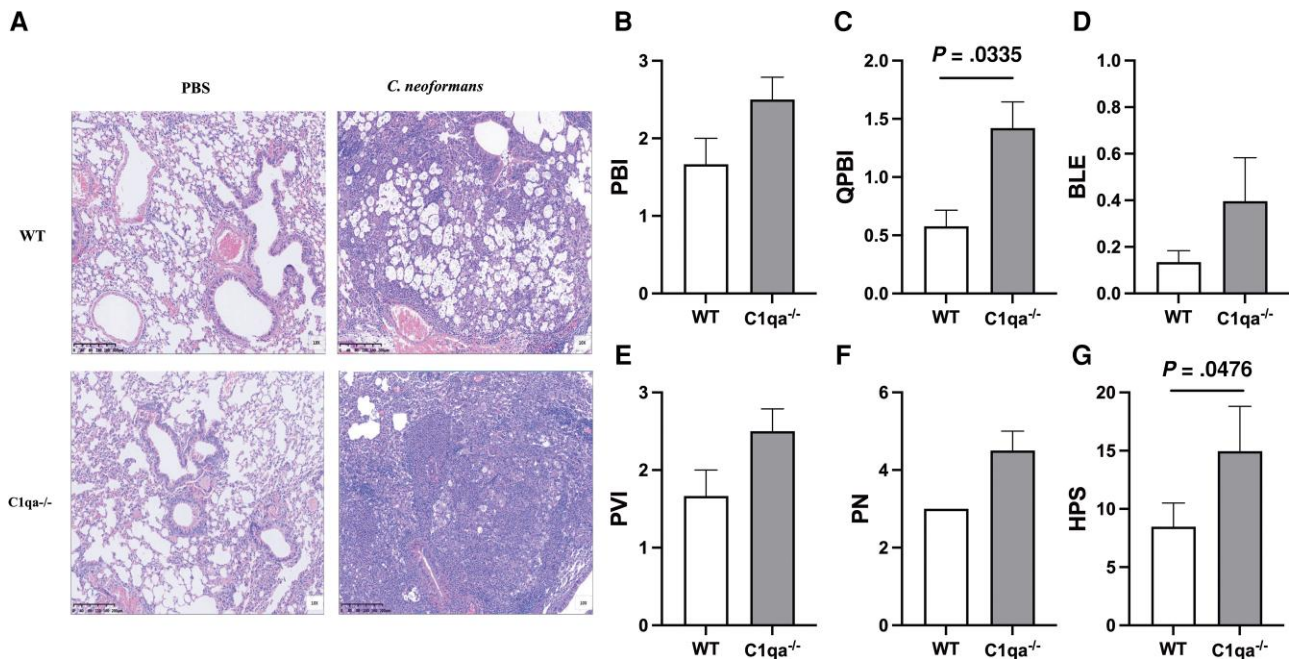
Figure 2. WT and $C1qa^{-/-}$ mice were intranasally administered PBS or 4×10^4 *C. neoformans* CFUs per mouse; they were killed at day 14 postinfection, and lungs were collected for H&E staining. *A*, Representative lung histopathology (×100). *B–G*, Quantification of *C. neoformans* infection induced histopathology including PBI, QPBI, BLE, PVI, PN, and HPS. Abbreviations: BLE, bronchiolar/bronchial luminal exudate; CFUs, colony-forming units; H&E, hematoxylin and eosin; HPS, histopathological score; PBI, peribronchiolar/bronchial infiltrated (percentage of sites); PBS, phosphate-buffered saline; PN, parenchymal pneumonia; PVI, perivascular infiltrate (percentage of sites); QPBI, quality of peribronchiolar/bronchial infiltrates; WT, wild-type; YPD, yeast extract-peptone-dextrose.

fungal pathogenicity during infection [20]. Indeed, we observed that a subset of cryptococcal cells in the lungs after 14 days of infection differentiated into giant cells in both WT and $C1qa^{-/-}$ mice (Figure 5A). Quantitative analysis showed that there were more Titan cells in the lungs of $C1qa^{-/-}$ mice compared with WT mice (Figure 5B). Next, we investigated whether the higher formation of Titan cells in the lungs of $C1qa^{-/-}$ mice was associated with some host-derived factors that were present in the lung of $C1qa^{-/-}$ mice. The prototype yeast cells H99 were cultured in vitro with lung homogenate supernatant obtained from WT and $C1qa^{-/-}$ mice that were infected with *C. neoformans* for 14 days. After incubation for 72 hours, although the $C1qa^{-/-}$ lung supernatant had no significant influence on the number of *C. neoformans* CFUs compared with WT lung supernatant (Figure 5C), cryptococcal cells cultured with supernatant from $C1qa^{-/-}$ mice displayed larger cell size and thicker capsule walls, exhibiting the properties of Titan cells. To determine whether C1q can inhibit the titanization of *C. neoformans*, we added human C1q protein to *Cryptococcus* incubated with 10% FCS. However, we found no significant difference compared with *Cryptococcus* incubated with only 10% FCS (Figure 5D). An analysis of the ratio of capsule to whole body size, which was related to the virulence of *C. neoformans*, showed that it was higher in the group cultured with lung supernatant from $C1qa^{-/-}$ mice compared

with the lung supernatant from WT mice (Figure 5E). Furthermore, culture medium supplemented with C1qa had no effect on Titan generation (data not shown), suggesting that C1qa regulated host factors, rather than C1qa itself, in the lung, which could influence the yeast-to-Titan transition.

C. neoformans isolated from the lung of $C1qa^{-/-}$ mice showed enhanced virulence in murine survival assays and more resistance to antimacrophage clearance in vitro.

Finally, we tested the virulence of *C. neoformans* isolated from the lung homogenates of $C1qa^{-/-}$ and WT mice by inoculating mice with these isolates. The lung homogenates from infected $C1qa^{-/-}$ mice and WT mice were cultivated on YPD plates. Interestingly, we observed that the size of *C. neoformans* cells was larger in the plates with lung homogenates from $C1qa^{-/-}$ mice than in those from WT mice (Figure 6A). One *C. neoformans* isolate was randomly harvested from plates cultured with lung homogenates of the infected WT or $C1qa^{-/-}$ mice and was referred to as the WT isolate or KO isolate, respectively. WT mice were infected with the same number of WT isolates or KO isolates and monitored for survival for 6 weeks. We found that 80% of mice infected with the KO isolate died by 42 days postinfection, at which time only 30% of mice had succumbed to infection with the WT isolate (Figure 6B). These results indicated that the lung environment of $C1qa^{-/-}$ mice might increase the virulence of the fungus by altering
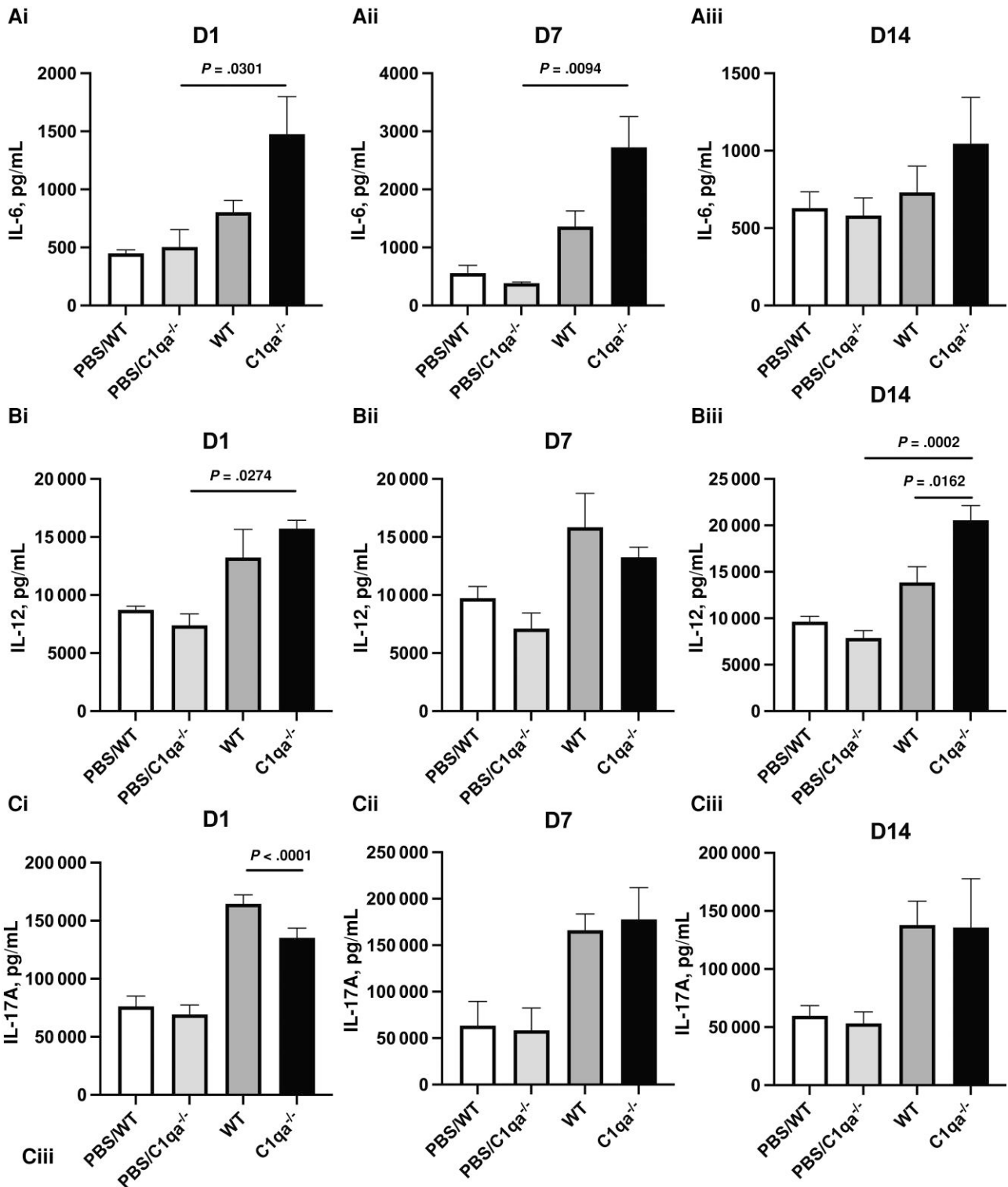
Figure 3. Lung cytokine analysis by ELISA after *C. neoformans* infection. *C1qa*$^{-/-}$ mice and WT mice were infected with 4×10^4 *C. neoformans* CFUs per mouse. The lungs were collected on days 1, 7, and 14 postinfection and homogenized. The concentrations of IL-6, IL-12, and IL-17A were measured in the supernatant of lung homogenates by ELISA. Abbreviations: CFUs, colony-forming units; ELISA, enzyme-linked immunosorbent assay; IL, interleukin.

hereditary material that could be transmitted to offspring cells. As the first line of defense, macrophage-mediated phagocytosis and killing play an important role in controlling fungal

infections [22]. To investigate whether the higher virulence of the KO isolate was due to resistance to antimacrophage clearance, macrophages were co-cultured with *Cryptococcus*,
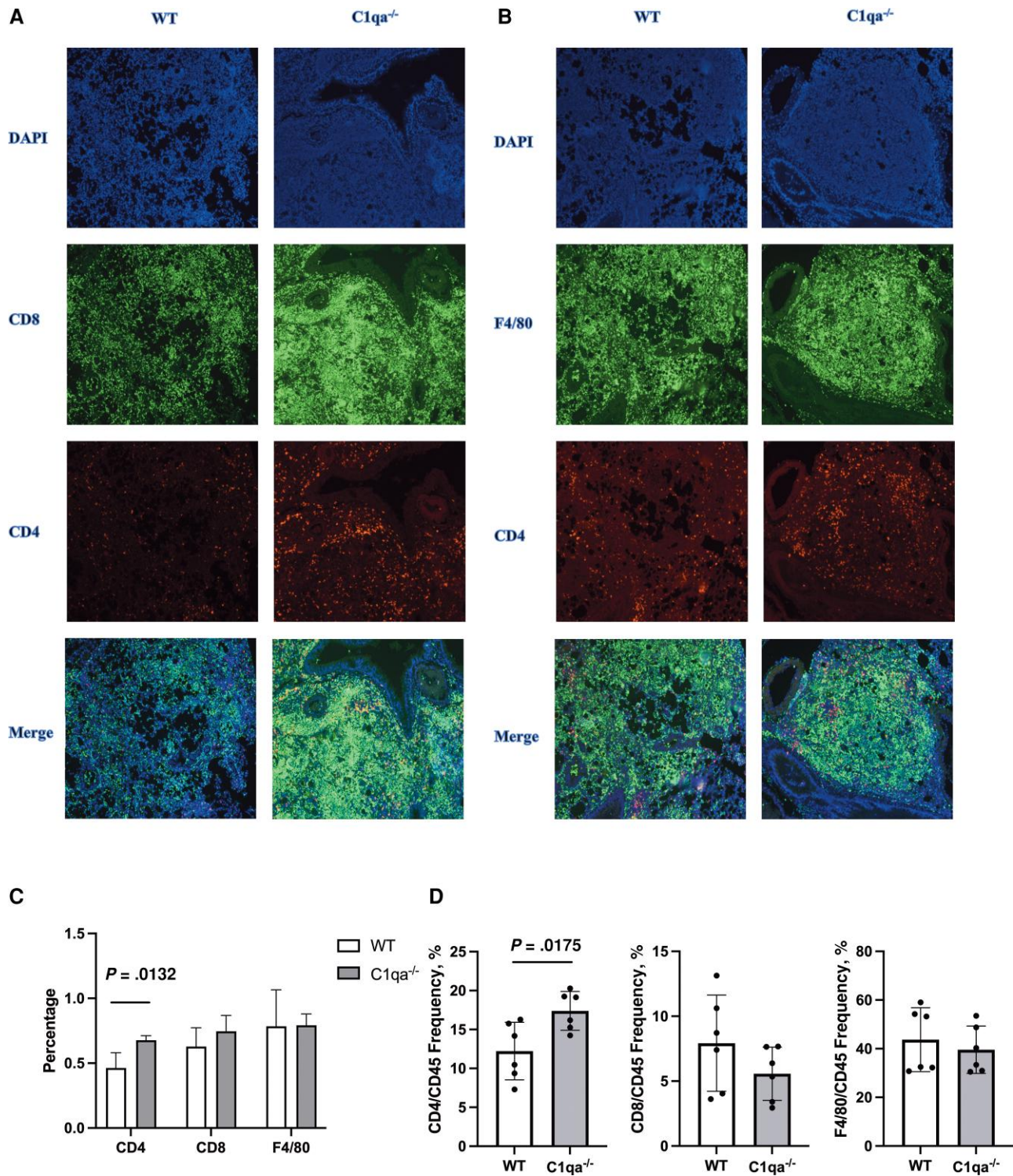
Figure 4. Analysis of CD4/CD8 T cells and macrophages in the lungs after *C. neoformans* infection by immunofluorescence staining. Mice were infected as described and killed on day 14 postinfection. *A*, Representative lung sections stained with CD4 and CD8 T cells. *B*, Representative lung images stained for CD4 and macrophages. *C*, The relative level of CD4/CD8 T cells and macrophages was quantified by fluorescence intensity. *D*, The relative level of CD4/CD8 T cells and macrophages was quantified by flow cytometry. Abbreviation: DAPI, 4′,6-diamidino-2-phenylindole.

including H99 (used as a control), WT isolate, or KO isolate for 18 hours with a multiplicity of infection of 10. The *Cryptococcus* cells in the culture medium and lysate of macrophages were combined, and their number was calculated by plate counting. The results showed that there was reduced killing of the KO isolate compared with both the H99 and WT isolates, while the WT
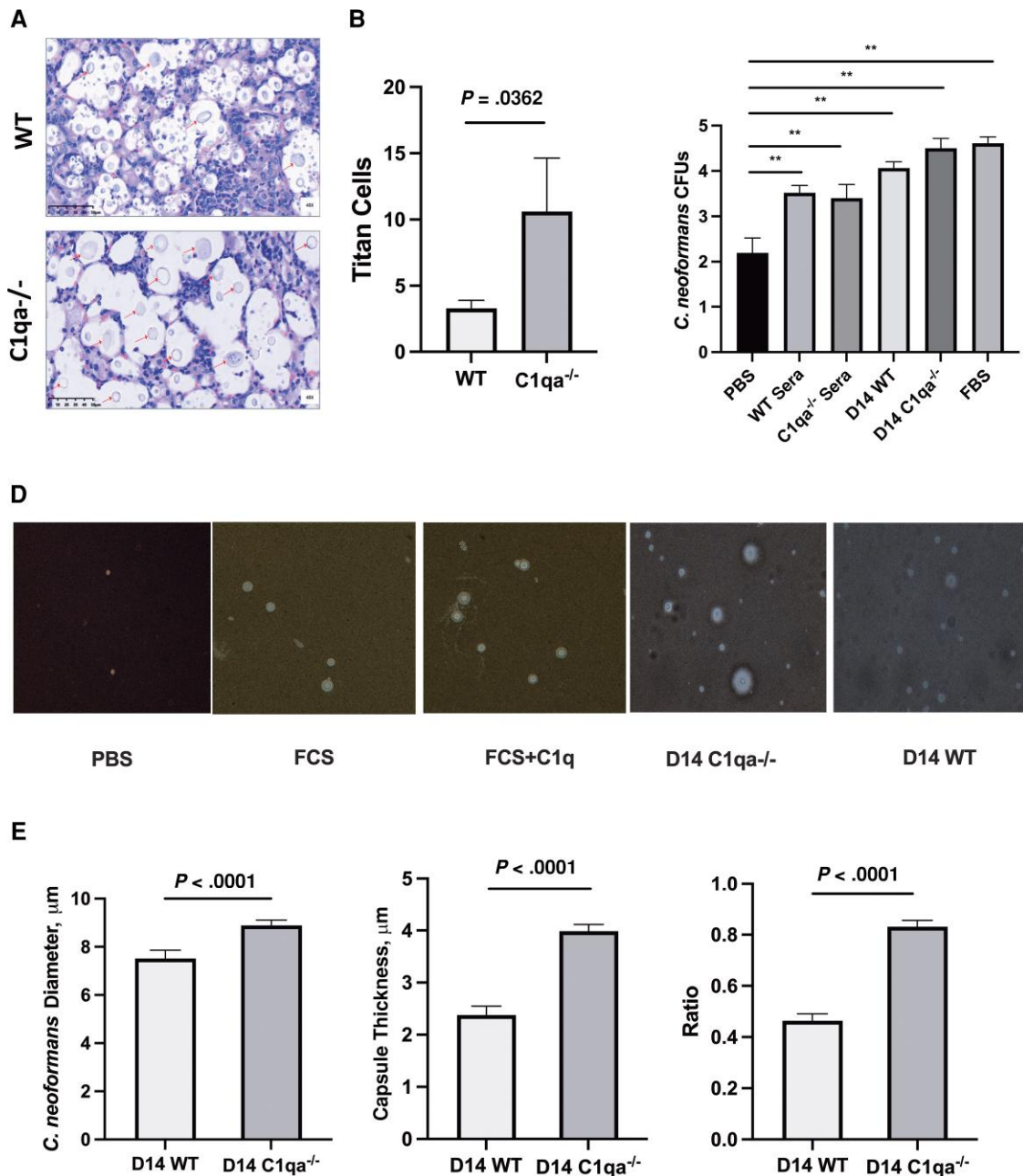
Figure 5. Enhanced Titan cell production in the lungs of $C1qa^{-/-}$ mice infected for 14 days. *A*, Representative lung images show giant *C. neoformans* (H&E, ×40). *B*, The Titan cells in the lungs were quantified as the average number of Titan cells per field. *C*, CFUs of *C. neoformans* co-cultured with PBS, sera from WT mice, sera from $C1qa^{-/-}$ mice, lung homogenate supernatant from WT and $C1qa^{-/-}$ mice, and FBS for 72 hours. **$P < .01$. *D*, Representative image of *C. neoformans* co-cultured with PBS, 10% FCS, 10% FCS + C1q, lung homogenate supernatant from WT, and $C1qa^{-/-}$ mice for 72 hours using microscopy. *E*, The size of the whole body of *C. neoformans* and the thickness of the capsule were measured, and the ratio of the capsule to the whole body of *C. neoformans* was calculated. Abbreviations: CFUs, colony-forming units; FCS, fetal calf serum; H&E, hematoxylin and eosin; PBS, phosphate-buffered saline; WT, wild-type.

isolate exhibited modest, nonsignificant resistance to macrophage killing compared with H99 (Figure 6C).

DISCUSSION

Here, we showed that during cryptococcal lung infection, although knockout of C1qa did not significantly increase fungal cell load in the lung and distribution in the tissue, it led to more severe pathological changes and lower survival rates of infected $C1qa^{-/-}$ mice, which had a higher inflammatory response and enhanced virulence of cryptococcal cells during infection.

C1q was first seen as a promoter of the classical complement pathway and plays an important role in anti-infection immunity. There are 3 activation pathways of the complement system
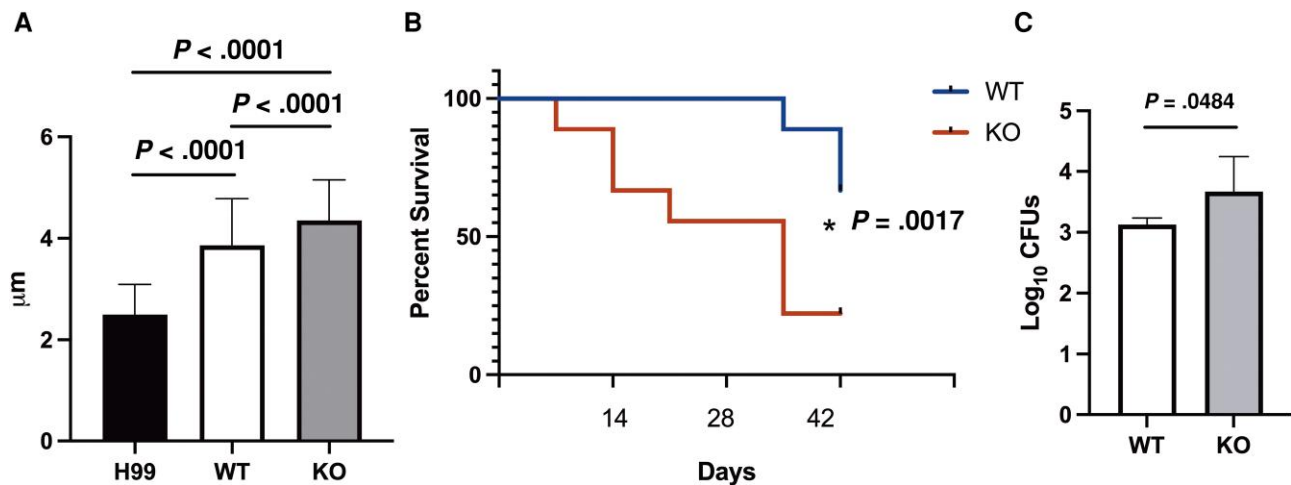
Figure 6. Mice infected with the WT isolate of *C. neoformans* have a lower mortality rate compared with the KO isolate, which exhibited higher resistance to macrophage killing in vitro. *A*, More large cells were observed in the KO isolate compared with the WT isolate ($P < .001$). *B*, Mice infected with the WT isolate of *C. neoformans* had a lower mortality rate than those infected with the KO isolate. *C*, The KO isolate showed higher resistance to macrophage killing than the WT isolate. The macrophages were incubated with the KO, WT, and H99 isolates for 18 hours. Abbreviations: KO, knockout; WT, wild-type.

(classical pathway, alternative, and lectin pathway). Our previous studies have shown that the lack of the classical pathway in C1qa-deficient mice does not affect the activation state of the other 2 pathways during pneumococcal infection [23]. In addition to mediating classical complement activation, many studies have shown the important role of C1q in immune regulation [24]. As a pattern recognition receptor (PRR) of the innate immune system, C1q could opsonize apoptotic cells and promote macrophage phagocytosis and suppress inflammatory responses [10]. Also, C1q has been reported to have a protective role in inflammatory diseases, such as atherosclerosis and Alzheimer's disease [16]. In our study, we found that there was an increased inflammatory response with increased levels of IL-6 and IL-12 and a reduced level of IL-17A in $C1qa^{-/-}$ mice on day 1. IL-12 is produced by dendritic cells and macrophages in response to infection and plays a critical role in activating T cells against infection. IL-6 is a pro-inflammatory cytokine that is produced by a variety of cells in response to infection, injury, or inflammation. It is possible that the differences in cytokine concentrations between the wild and C1qa-deficient mice during cryptococcal lung infection may be due to a complex interplay between immune cell activation, *C. neoformans* strain virulence, and regulatory mechanisms. The specific mechanisms underlying these differences would require further investigation.

Considering that $C1qa^{-/-}$ mice exhibited a similar fungal load in the tissue compared with WT mice, we speculated that C1qa may directly involve the regulation of immune cell function to control inflammatory response during cryptococcal infection and the increased formation of virulent fungal cells that might aggravate pathological changes. The detailed mechanisms of how C1qa participates in the inflammatory pathway and what kinds of immune cells are regulated by C1qa need to be studied in the future.

The pathogenic *C. neoformans* cells can switch to a morphotype termed Titan cell in response to environmental stimuli in the lung [25, 26]. Accompanied by these morphogenic transitions, *C. neoformans* enhances their virulence, drives pathogenesis, and resists host elimination to prolong infection [17]. For example, Ivy M. Dambuza has reported that *C. neoformans* titanization created variance in body size and capsule thickness in response to environmental stimuli [17]. Such a morphological transition could not only drive pathogenesis and niche adaptation, but also have a significant impact on the initiation and maintenance of *C. neoformans* infections [27, 28]. Our study also observed that Titan cells were predominantly in the lung after 14 days postinfection. Interestingly, deficiency of C1qa promoted generation of Titan cells in the lung that was associated with enhanced lung inflammation. However, C1q has no direct effect on *Cryptococcus* titanization in vitro. One explanation is that loss of C1qa results in dysregulation of inflammation during *C. neoformans* infection, leads to enhanced inflammation in the lung, and consequently promotes fungi to switch to a resistant yeast form. Of course, it is also possible that the increased inflammation and more severe disease outcomes observed in $C1qa^{-/-}$ mice are due to the production of more Titan cells in the lung of $C1qa^{-/-}$ mice. Our current study presents a reproducible in vitro system to generate all properties of Titan cells by using lung homogenate supernatant; more importantly, we showed that this system by using lung homogenate supernatant recapitulates the in vivo observation that more Titan cells were generated in the lung

environment of $C1qa^{-/-}$ mice compared with WT mice. Metabolomics analysis may be used to measure the host-derived factors in the lung homogenate supernatant that differentially present in WT and $C1qa^{-/-}$ mice and to reveal the candidate factors that promote the generation of Titan cells in $C1qa^{-/-}$ mice during *C. neoformans* infection.

Pathogens rely on the expression of virulence factors to reach specialized niches to replicate. However, virulence factors are often tightly regulated to adapt to specific environments to promote pathogen fitness [29]. Many studies have shown that attenuated strains of pathogens were selected in the host during infection [29]. These attenuated strains could asymptomatically and persistently colonize the primary host, and the attenuated virulent phenotype could be transmitted to their offspring cells, which were able to persistently and asymptomatically colonize new hosts [30]. In our current study, we found that deficiency in C1qa promoted the generation of the virulent form of *Cryptococcus* cells, and this phenotype could be transmitted to offspring fungal cells that were more resistant to macrophage killing in vitro and caused a lower survival rate of mice during these offspring fungal infections. This result indicated that the lung microenvironment in C1qa-deficient mice not only changed the morphology of *C. neoformans* but also promoted the selection of strains with mutations in genes that enhance its virulence, although this needs to be confirmed by performing whole-genome sequencing of the KO isolates in future studies. We acknowledge that although we showed that mice infected with the KO isolate from C1qa-deficient mice had a lower survival rate compared with WT mice, we did not explore the mechanism of the virulent difference between isolates from $C1qa^{-/-}$ mice and WT mice in the murine model, for example, whether their virulence differences are associated with the alteration of fungal burdens and inflammation in the tissue or Titan cell formation. Macrophages play an important role in controlling *Cryptococcus* infection, while in many cases macrophages could be the shelter of *Cryptococcus* to escape the attack of the body's immune system. *Cryptococcus* could survive in the macrophages, proliferate, and spread. Our in vitro macrophage killing assay showed that the KO isolates have a stronger antimacrophage clearance ability than WT isolates, suggesting that increasing antimacrophage clearance ability is at least one of the factors that contributes to increased virulence in KO isolates.

Our data serve as the first example of the interaction between host C1q and fungus in the lung that mediates fungal morphological transitions, virulence changes, and alterations of their pathogenesis. Our current research is based on observation of the H99 strain infecting both WT and $C1qa^{-/-}$ mice, and we documented some interesting phenomena. In the future, more types of strains will be observed to determine whether such changes are a common phenomenon. The relative importance of immune status to the alteration of *Cryptococcus* morphology and virulence needs to be investigated in the future, especially in the context of clinically relevant, immune-altered states, including T- and B-cell deficiency and neutropenia.

Supplementary Data

Acknowledgments

References

1. Kwon-Chung KJ, Fraser JA, Doering TL, et al. *Cryptococcus neoformans* and *Cryptococcus gattii*, the etiologic agents of cryptococcosis. Cold Spring Harb Perspect Med **2014**; 4:a019760.
2. Garcia-Rodas R, de Oliveira HC, Trevijano-Contador N, Zaragoza O. Cryptococcal titan cells: when yeast cells are all grown up. Curr Top Microbiol Immunol **2019**; 422:101–20.
3. Okagaki LH, Nielsen K. Titan cells confer protection from phagocytosis in *Cryptococcus neoformans* infections. Eukaryot Cell **2012**; 11:820–6.
4. Choi J, Vogl AW, Kronstad JW. Regulated expression of cyclic AMP-dependent protein kinase A reveals an influence on cell size and the secretion of virulence factors in *Cryptococcus neoformans*. Mol Microbiol **2012**; 85:700–15.
5. Franzot SP, Mukherjee J, Cherniak R, Chen LC, Hamdan JS, Casadevall A. Microevolution of a standard strain of *Cryptococcus neoformans* resulting in differences in virulence and other phenotypes. Infect Immun **1998**; 66:89–97.
6. Crabtree JN, Okagaki LH, Wiesner DL, Strain AK, Nielsen JN, Nielsen K. Titan cell production enhances the virulence of *Cryptococcus neoformans*. Infect Immun **2012**; 80:3776–85.
7. Brown SM, Campbell LT, Lodge JK. *Cryptococcus neoformans*, a fungus under stress. Curr Opin Microbiol **2007**; 10:320–5.
8. Garcia-Barbazan I, Trevijano-Contador N, Rueda C, et al. The formation of titan cells in *Cryptococcus neoformans* depends on the mouse strain and correlates with induction of th2-type responses. Cell Microbiol **2016**; 18:111–24.
9. Pirofski LA. Of mice and men, revisited: new insights into an ancient molecule from studies of complement activation by *Cryptococcus neoformans*. Infect Immun **2006**; 74:3079–84.
10. Rohatgi S, Pirofski LA. Host immunity to *Cryptococcus neoformans*. Future Microbiol **2015**; 10:565–81.
11. Kouser L, Madhukaran SP, Shastri A, et al. Emerging and novel functions of complement protein C1q. Front Immunol **2015**; 6:317.
12. Benoit ME, Clarke EV, Morgado P, Fraser DA, Tenner AJ. Complement protein C1q directs macrophage polarization and limits inflammasome activity during the uptake of apoptotic cells. J Immunol **2012**; 188:5682–93.
13. Fraser DA, Laust AK, Nelson EL, Tenner AJ. C1q differentially modulates phagocytosis and cytokine responses during ingestion of apoptotic cells by human monocytes, macrophages, and dendritic cells. J Immunol **2009**; 183:6175–85.
14. Botto M, Dell'Agnola C, Bygrave AE, et al. Homozygous C1q deficiency causes glomerulonephritis associated with multiple apoptotic bodies. Nat Genet **1998**; 19:56–9.

15. Taylor PR, Carugati A, Fadok VA, et al. A hierarchical role for classical pathway complement proteins in the clearance of apoptotic cells in vivo. J Exp Med **2000;** 192:359–66.

16. Geunes-Boyer S, Beers MF, Perfect JR, Heitman J, Wright JR. Surfactant protein D facilitates *Cryptococcus neoformans* infection. Infect Immun **2012;** 80: 2444–53.

17. Zou J, Reddivari L, Shi Z, et al. Inulin fermentable fiber ameliorates type I diabetes via IL22 and short-chain fatty acids in experimental models. Cell Mol Gastroenterol Hepatol **2021;** 12:983–1000.

18. Cimolai N, Taylor GP, Mah D, Morrison BJ. Definition and application of a histopathological scoring scheme for an animal model of acute *Mycoplasma pneumoniae* pulmonary infection. Microbiol Immunol **1992;** 36:465–78.

19. da Silva-Junior EB, Firmino-Cruz L, Guimaraes-de-Oliveira JC, et al. The role of toll-like receptor 9 in a murine model of *Cryptococcus gattii* infection. Sci Rep **2021;** 11:1407.

20. Dambuza IM, Drake T, Chapuis A, et al. The *Cryptococcus neoformans* titan cell is an inducible and regulated morphotype underlying pathogenesis. PLoS Pathog **2018;** 14:e1006978.

21. Shen L, Zheng J, Wang Y, et al. Increased activity of the complement system in cerebrospinal fluid of the patients with non-HIV cryptococcal meningitis. BMC Infect Dis **2017;** 17:7.

22. Brown GD. Innate antifungal immunity: the key role of phagocytes. Annu Rev Immunol **2011;** 29:1–21.

23. Li Q, Li YX, Stahl GL, Thurman JM, He Y, Tong HH. Essential role of factor B of the alternative complement pathway in complement activation and opsonophagocytosis during acute pneumococcal otitis media in mice. Infect Immun **2011;** 79:2578–85.

24. Espericueta V, Manughian-Peter AO, Bally I, Thielens NM, Fraser DA. Recombinant C1q variants modulate macrophage responses but do not activate the classical complement pathway. Mol Immunol **2020;** 117:65–72.

25. Gerstein AC, Fu MS, Mukaremera L, et al. Polyploid titan cells produce haploid and aneuploid progeny to promote stress adaptation. mBio **2015;** 6:e01340-15.

26. Zaragoza O, Garcia-Rodas R, Nosanchuk JD, Cuenca-Estrella M, Rodriguez-Tudela JL, Casadevall A. Fungal cell gigantism during mammalian infection. PLoS Pathog **2010;** 6:e1000945.

27. Feldmesser M, Kress Y, Casadevall A. Dynamic changes in the morphology of *Cryptococcus neoformans* during murine pulmonary infection. Microbiology (Reading) **2001;** 147:2355–65.

28. Okagaki LH, Strain AK, Nielsen JN, et al. Cryptococcal cell morphology affects host cell interactions and pathogenicity. PLoS Pathog **2010;** 6:e1000953.

29. An J, Zhao X, Wang Y, Noriega J, Gewirtz AT, Zou J. Western-style diet impedes colonization and clearance of *Citrobacter rodentium*. PLoS Pathog **2021;** 17: e1009497.

30. Sanchez KK, Chen GY, Schieber AMP, et al. Cooperative metabolic adaptations in the host can favor asymptomatic infection and select for attenuated virulence in an enteric pathogen. Cell **2018;** 175:146–58.e15.